

## Original Research Article

# Evaluation of plan adaptation strategies for stereotactic radiotherapy of lymph node oligometastases using online magnetic resonance image guidance



Dennis Winkel\*, Gijsbert H. Bol, Anita M. Werensteijn-Honingh, Ilse H. Kiekebosch, Bram van Asselen, Martijn P.W. Intven, Wietse S.C. Eppinga, Bas W. Raaymakers, Ina M. Jürgenliemk-Schulz, Petra S. Kroon

Department of Radiotherapy, University Medical Center, Utrecht, the Netherlands

## ARTICLE INFO

## Keywords:

Lymph node oligometastases  
MR-guided radiotherapy  
Online plan adaptation  
Mr-linac  
Igrt

## ABSTRACT

**Background and purpose:** Recent studies have shown that the use of magnetic resonance (MR) guided online plan adaptation yields beneficial dosimetric values and reduces unplanned violations of the dose constraints for stereotactic body radiation therapy (SBRT) of lymph node oligometastases. The purpose of this R-IDEAL stage 0 study was to determine the optimal plan adaptation approach for MR-guided SBRT treatment of lymph node oligometastases.

**Materials and Methods:** Using pre-treatment computed tomography (CT) and repeated MR data from five patients with in total 17 pathological lymph nodes, six different methods of plan adaptation were performed on the daily MRI and contours. To determine the optimal plan adaptation approach for treatment of lymph node oligometastases, the adapted plans were evaluated using clinical dose criteria and the time required for performing the plan adaptation.

**Results:** The average time needed for the different plan adaptation methods ranged between 11 and 119 s. More advanced adaptation methods resulted in more plans that met the clinical dose criteria [range, 0–16 out of 17 plans]. The results show a large difference between target coverage achieved by the different plan adaptation methods.

**Conclusion:** Results suggested that multiple plan adaptation methods, based on plan adaptation on the daily anatomy, were feasible for MR-guided SBRT treatment of lymph node oligometastases. The most advanced method, in which a full online replanning was performed by segment shape and weight optimization after fluence optimization, yielded the most favourable dosimetric values and could be performed within a time-frame acceptable (< 5 min) for MR-guided treatment.

## 1. Introduction

Image-guided radiation therapy (IGRT) [1] has vastly developed over the past decades and is currently indispensable in modern radiation therapy to reduce the effect of setup errors and geometrical variations of the target volume and organs at risk (OARs). To visualize the target volume and surrounding tissues prior to treatment, techniques such as portal imaging and cone-beam computed tomography (CBCT) are often used [2,3]. These techniques have greatly contributed towards precision radiotherapy, but yield relatively poor soft tissue contrast which can make it challenging to accurately identify the target. To resolve this problem bony anatomy or implanted fiducial markers are often used as

surrogate for position verification of the target [4–6].

Magnetic resonance (MR) guided radiotherapy systems are becoming increasingly available and are introduced in clinical practice [7–9]. Compared to linear accelerators with CBCT, these MR-guided systems provide a better soft tissue contrast which allows incorporation of more detailed patient anatomical information in the radiotherapy treatment plan [10,11]. One of these MR-guided systems is the 1.5 T MR-linac, which is able to provide diagnostic quality imaging of the patient anatomy during radiation therapy [12]. This enables accurate identification of the target volume, as well as the OARs and other surrounding tissues, and offers opportunities for online plan adaptation using the actual patient anatomy [13]. However, to be able to perform plan adaptation on the actual patient

\* Corresponding author. at: University Medical Center Utrecht, Department of Radiotherapy, Q.00.3.11, P.O. Box 85500, 3508 GA Utrecht, The Netherlands.  
E-mail address: [d.winkel-2@umcutrecht.nl](mailto:d.winkel-2@umcutrecht.nl) (D. Winkel).

anatomy, multiple additional, and potentially time-consuming, steps are required. After obtaining online imaging, it must be registered with pre-treatment imaging. Deformable image registration is required to propagate the contours, after which they must be evaluated and potentially corrected. Because a new plan is created, plan quality assurance (QA) should be performed prior to delivery [9,14].

Local treatment of lymph node oligometastases is commonly performed using stereotactic body radiation therapy (SBRT) [15–17]. In SBRT a relatively high irradiation dose is delivered in a limited number of fractions to the target in a highly conformal manner with steep dose gradients to achieve good sparing of the OARs [18,19]. To keep treatment volumes as small as possible and minimize the amount of normal tissue that is irradiated, good target visualization during treatment is necessary in SBRT [20]. When using SBRT for the treatment of lymph node oligometastases good online target visualisation is needed to deal with inter-fraction changes in shape and size of the target and OARs and different positions of the target relative to OARs [21]. MR-guided online adaptive radiotherapy is clinically deliverable and safe and allows for dose escalation and OARs sparing compared to non-adaptive abdominal SBRT [22].

Recent studies have shown that the use of MR-guided online plan adaptation, taking daily anatomical variations into account, yields beneficial dosimetric values and reduces the amount of unplanned violations of the dose constraints [20,23]. While the dosimetric benefit is already shown, there are multiple approaches for MR-guided online plan adaptation, based on contours generated on the daily anatomy, to be explored.

Although it is evident that a high plan quality is always preferred, time is also a limiting factor to keep total treatment time within 45 min, which is considered acceptable. With this in mind, online plan adaptation should preferably be performed within five minutes. The purpose of this R-IDEAL stage 0 [24] study was to evaluate different plan adaptation strategies to determine the optimal plan adaptation approach for MR-guided SBRT treatment of lymph node oligometastases.

## 2. Materials and methods

### 2.1. Patient data

Pre-treatment computed tomography (CT) and sequential magnetic resonance imaging (MRI) data from five female patients with locally advanced cervical cancer with in total 17 pelvic and *para*-aortic pathological lymph nodes was used. All patients were treated with chemoradiation with curative intention and an additional MRI was acquired during the first three weeks of treatment. This patient data, which was used as a test case, did not contain real oligometastatic state. Because of the palliative intent of this treatment, we don't want to place any additional load on patients with lymph node oligometastases with additional imaging. It is expected for lymph nodes and surrounding OARs to behave similar in oligometastatic state. MRI was acquired on a 1.5 T Philips Ingenia using a mDIXON 3D FFE T1W sequence (flip angle 10°; TE1/TE2 = 1.6/3.9 ms, TR = 5.7 ms, reconstructed voxel  $1.05 \times 1.05 \times 2.5 \text{ mm}^3$ , FOV  $552 \times 552 \times 300 \text{ mm}^3$ ) during free breathing and was used for delineation. Patient preparation and motion management was equal for all image acquisition. The acquisition time (approximately six minutes) and image quality of these scans are comparable to the 1.5 T MR-linac (Unity, Elekta AB, Stockholm, Sweden). All lymph node metastases and OARs on the pre-treatment CT and MRI scans were delineated by an experienced radiation oncologist treating lymph node oligometastases. The mean gross target volume (GTV) of the lymph nodes was  $2.5 \pm 2.8 \text{ cm}^3$  (1 SD) [range, 0.4–15.8  $\text{cm}^3$ ]. All patients gave written informed consent.

### 2.2. Pre-treatment plan generation

A pre-treatment plan for each of the 17 individual lymph nodes was generated on the pre-treatment CT with a prescribed dose of 5x7Gy to

**Table 1**

Clinical dose criteria for SBRT lymph node oligometastases plans for five fractions as used in the evaluation of the treatment plans, based on the UK SABR consortium guidelines (2016).

Structure	Constraint
PTV	$V_{35\text{Gy}} > 95\%$
Bladder	$D_{\text{max}} < 47.25 \text{ Gy}$
	$D_{0.5\text{cm}^3} < 38 \text{ Gy}$
	$D_{1.5\text{cm}^3} < 18.3 \text{ Gy}$
Bowel, Rectum, Sigmoid	$D_{0.5\text{cm}^3} < 35 \text{ Gy}$
	$D_{1\text{cm}^3} < 25 \text{ Gy}$

the target, using a 3 mm isotropic planning target volume (PTV) margin which will be used in our clinical protocol. Using a vacuum cushion for immobilization, these PTV margins are considered to be sufficient to handle patient setup, intra-fraction motion and machine related uncertainties [9,25–29]. All plans were generated using Monaco (Version 5.40.00 build 19, Elekta AB, Sweden) treatment planning software (TPS) with the MR-linac machine model and a 1.5 T magnetic field in superior-inferior patient direction. The hardware used consists of an Intel Xeon E5-2960 CPU, 128 GB RAM and two Nvidia Quadro GP100 GPU's. OAR dose was lowered as much as possible, while maintaining a sufficient PTV coverage of  $V_{35\text{Gy}} > 95\%$ . Clinical dose criteria for the OARs were based on the UK SABR consortium guidelines (2016) (Table 1). The plans were generated for intensity modulated radiotherapy (IMRT) with a maximum of 45 segments and a minimum of five monitor units per segment. Seven gantry angles were selected depending on the location of the target [30]. For left sided targets, the following gantry angles were used: 0°, 30°, 60°, 90°, 114°, 144° and 174°. For right sided targets, the used gantry angles were mirrored: 0°, 330°, 300°, 270°, 246°, 216° and 186°. All dose calculation was performed using the GPUMCD [31] dose engine available in Monaco TPS with a statistical uncertainty of 3% per control point. A calculation grid size of 3 mm was used to increase optimization speed, which was resampled by the TPS to a grid size of 1 mm for accurate dosimetric evaluation after optimization.

### 2.3. Plan adaptation strategies

Plan adaptation was performed using the plan from the pre-treatment CT and daily MRI and contours. Both data sets were automatically registered with each other by rigid registration based on mutual information [32] and the contours were automatically propagated by deformable registration using the Monaco TPS. Electron densities were assigned per structure based on the average ED value of the corresponding contour on the pre-treatment CT. No overrides were used for structures for either the pre-treatment CT and daily MR. After these steps it was possible to perform plan adaptation on the new anatomy using one of the following six plan adaptation methods available in the adapt to shape workflow, which enables online plan adaptation on daily contours (Fig. 1):

- Original Segments
- Adapt Segments
- Optimize Weights from segments
- Optimize Weights from fluence
- Optimize Weights and Shapes from segments
- Optimize Weights and Shapes from fluence

The Original Segments (A) method makes use of the segments and monitor units (MUs) from the pre-treatment plan, and only the plan isocenter is modified. Herewith, the original plan is calculated on the daily anatomy. The Adapt Segments (B) method shifts the segments from the pre-treatment plan relative to the isocenter, based on the registration between the pre-treatment and online images, using Segment

## Methods for plan adaptation on daily anatomy and contours for the 1.5T MR-linac

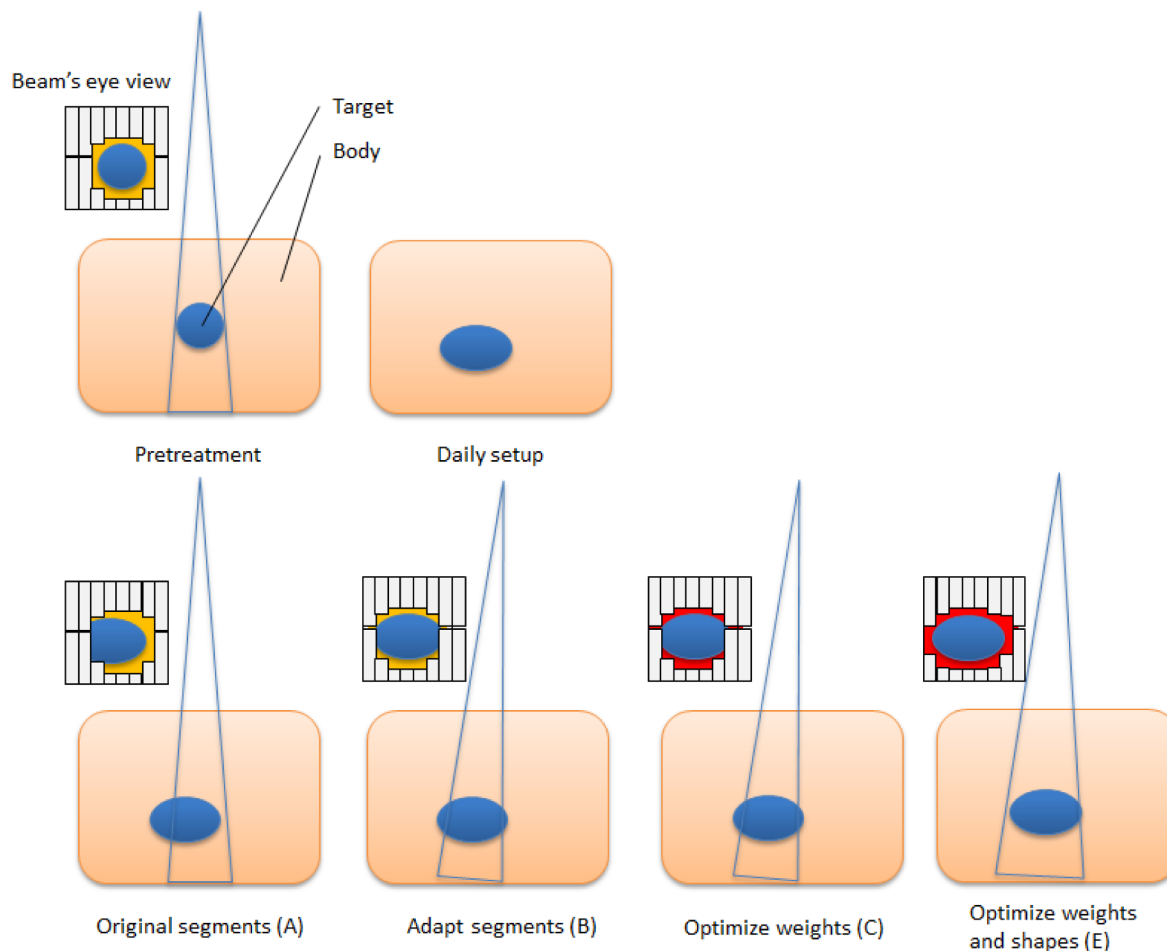


**Fig. 1.** Schematic overview of the segment changes for the different plan adaptation methods available in the treatment planning software for the 1.5 T MR-linac for plan adaptation on the daily anatomy and contours. A different background color (e.g. red or yellow) in the Beam's eye view (BEV) indicates a different segment weighting. When performing plan adaptation methods using optimize weights (method D) or optimize weights and shapes (method F) starting with full fluence optimization, the original segments are discarded and new initial plan segmentation is performed. (For interpretation of the references to color in this figure legend, the reader is referred to the web version of this article.)

Aperture Morphing (SAM) [33]. Using the resulting segments, the dose is calculated on the daily anatomy. Both Optimize Weights (C,D) methods are based on optimizing the weights of the segments for the daily anatomy by adjusting the amount of MUs. Method C optimizes the weights, using the set of segments from the pre-treatment plan after SAM. With method D the fluence is first re-optimized and a new set of segments is created. The new set of segments is then further optimized using segment weight optimization. The same distinction applies for both Weights and Shapes (E,F) methods. Either the pre-treatment segments are used (after SAM) for weight and shape optimization (method E), or a fluence re-optimization is performed and the new set of segments is optimized for the daily anatomy situation using both segment weight optimization, adjusting the amount of MUs, and segment shape optimization. So for method A, B, C and E, the segments from the pre-treatment plan are used for input and for method D and F, a new set of segments is created based on the re-optimized fluence. Method F, in which first the fluence is re-optimized and segmented and afterwards segment weight and shape optimization is performed, is equal to full online replanning. The plan is optimized towards the original planning constraints. No additional manual planning was performed.

### 2.4. Evaluation

To determine the optimal plan adaptation approach, the plans were

evaluated based on the optimization time required for the plan adaptation and the clinical dose criteria (Table 1) for the PTV coverage and surrounding OARs: bladder, bowel, rectum and sigmoid. The average time required for plan adaptation will be reported with one standard deviation (SDV).

### 3. Results

The median PTV on the daily MR was 99% [range, 90–105%] of the PTV on the pre-treatment CT. The average calculation time needed for the different plan adaptation methods ranged between 11 and 119 s. More advanced adaptation methods resulted in more plans that met the clinical dose criteria [range, 0–16 out of 17 plans](Fig. 2). The results showed a difference between target coverage achieved by the different plan adaptation methods (Fig. 3). Differences in dose to the OARs between the pre-treatment plan and different plan adaptation methods occurred. The largest differences occurred using method A. Methods B-F showed large similarities (Fig. 4). Finally, the times for plan adaptation increased when more complex plan adaptation methods were used (Fig. 5).

For the pre-treatment plans 16 out of 17 (94%) met all clinical dose criteria. For one plan it was not possible to achieve sufficient target coverage, without violating dose criteria for the OARs. This particular plan resulted in a PTV  $V_{35Gy}$  of 84%. The median PTV  $V_{35Gy}$  for all pre-

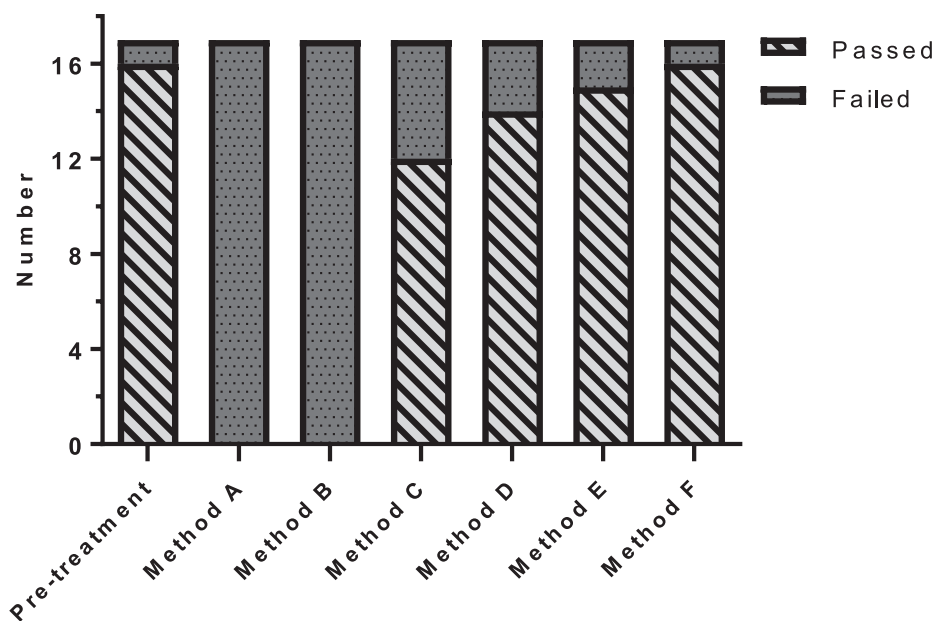


**Fig. 2.** Number of plans (N = 17 lymph nodes) that met all dose criteria based on the UK SABR consortium guidelines and a prescribed dose of  $V_{35Gy} > 95\%$  for plan adaptation on the daily anatomy and contours for the 1.5T MR-linac. Method A – F describe: A the original segments, B adapt segments, C optimize weights from segments, D optimize weights from fluence, E optimize weights and shapes from segments and F optimize weights and shapes from fluence, respectively.

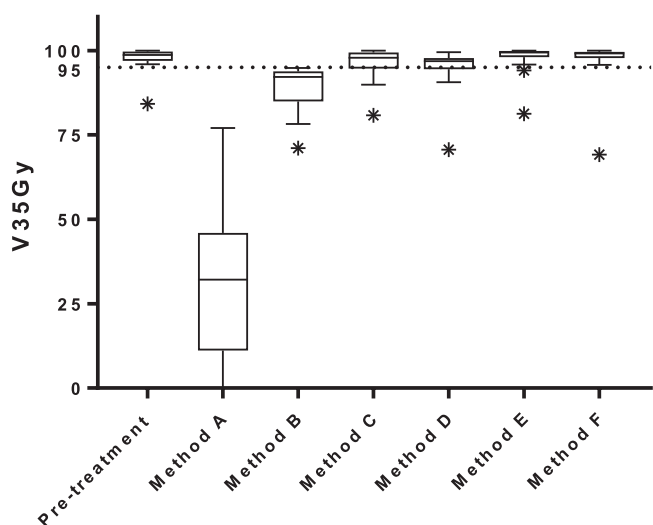


**Fig. 3.** Boxplot of the target dose coverage (N = 17 lymph nodes) described as planning target volume (PTV)  $V_{35Gy}$  in % for plan adaptation on the daily anatomy and contours for the 1.5T MR-linac. The 95% line depicts the minimum target coverage following the clinical dose constraints. The bars show the upper and lower quartiles. The whiskers show the minimum and maximum values, excluding outliers which are denoted with an asterisk. Method A – F describe: A the original segments, B adapt segments, C optimize weights from segments, D optimize weights from fluence, E optimize weights and shapes from segments and F optimize weights and shapes from fluence, respectively.

treatment plans was 99% [84 – 100%].

Plan adaptation using method A: the Original Segments method did not result in any plans that met clinical dose criteria. The target coverage was poor with a median PTV  $V_{35Gy}$  of 32 [0–77%]. In addition, violations to the OARs were present. One plan had violations of both the  $D_{0.5cm^3}$  and  $D_{15cm^3}$  of the bladder with 38.2 Gy and 18.7 Gy, respectively. The same plan also had a violation of the  $D_{0.5cm^3}$  of the sigmoid with a value of 36.3 Gy. Two other plans had a violation of the  $D_{0.5 cm^3}$  of the bowel with values of 36.5 Gy in one plan and 36.2 Gy in the other plan. Performing plan adaptation using this method took on average  $11 \pm 3$  s.

Using the Adapt Segments method (method B) did not result in any plans that had sufficient target coverage, however the coverage was

higher compared to the previously described Original Segments method with a median PTV  $V_{35Gy}$  of 92% [71–95%]. Although target coverage was insufficient in all plans, 11/17 (65%) of the plans had a PTV  $V_{35Gy}$  of > 90% and were thereby close to an acceptable target coverage of > 95%. The clinical dose criteria for the OARs were met in all 17 plans. Using this method plan adaptation took  $11 \pm 2$  s on average.

The Optimize Weights from segments method (method C) resulted in 12/17 (71%) plans that met all clinical dose criteria. In four plans the PTV  $V_{35Gy}$  was insufficient with values of 80%, 90%, 92% and 94%. One of these plans also had a violation of the  $D_{0.5cm^3}$  of the bowel with a value of 35.6 Gy. The remaining plan that did not meet the clinical dose criteria had a violation of the maximum dose in the PTV which was 47.7 Gy. The average time for plan adaptation using this method was  $19 \pm 3$  s.

With method D, the Optimize Weights from fluence method, 14/17 (82%) plans met all clinical dose criteria. Three plans violated the dose criteria with regards to the target coverage with a PTV  $V_{35Gy}$  of 71%, 91% and 93%. The clinical dose constraints for the OARs were not violated. Using this method for plan adaptation took  $25 \pm 5$  s on average.

Plan adaptation with the optimize weights and shapes method (method E), using the original segments, resulted in 15/17 (88%) plans that met all clinical dose criteria. The two plans that did not meet the clinical dose criteria had insufficient target coverage with a PTV  $V_{35Gy}$  of 81% and 94%. As for the previous method, no violations of the clinical dose constraints for the OARs were found. Plan adaptation using this method took  $112 \pm 26$  s on average.

Using the optimize weights and shapes method (method F), after full fluence re-optimization, 16/17 (94%) of all plans met clinical dose criteria. One plan, which did also not meet sufficient target coverage during pre-treatment planning, did not meet the constraint for the PTV  $V_{35Gy}$  with a value of 69%. Using this method, which is a full online replanning, optimization took  $119 \pm 22$  s on average.

#### 4. Discussion

This study shows that it is feasible to perform online plan adaptation for MR-guided SBRT treatment of lymph node oligometastases using different plan adaptation methods. The Original Segments method (method A) did not result in suitable plans, which was expected because even the slightest positioning error or inter-fraction motion with regards to the pre-treatment plan would mean that the treatment plan

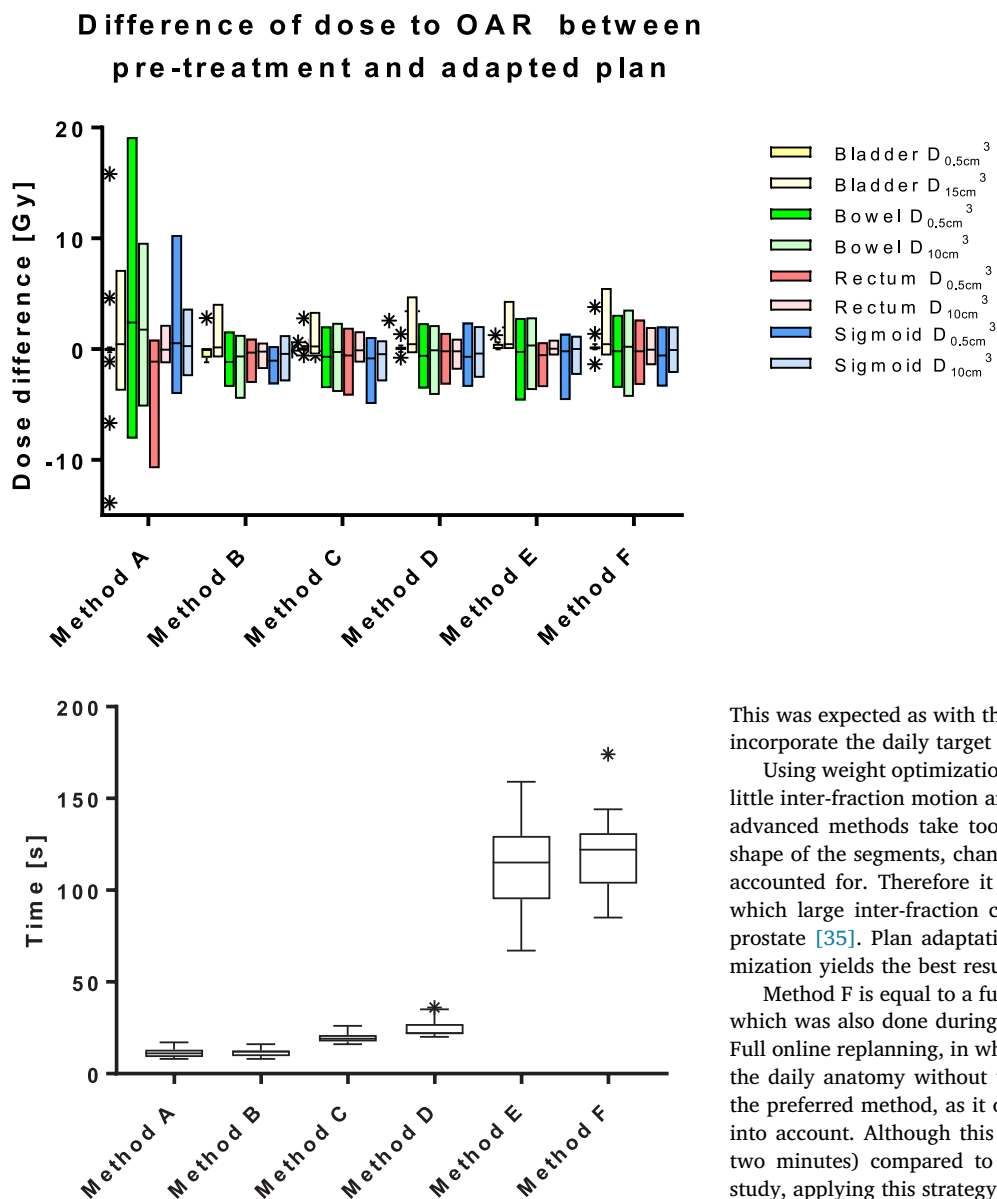


Fig. 5. Boxplot of the measured time in seconds for each different plan adaptation method (N = 17 lymph nodes) for plan adaptation on the daily anatomy and contours for the 1.5 T MR-linac. The bars show the upper and lower quartiles. The whiskers show the minimum and maximum values, excluding outliers which are denoted with an asterisk. Method A – F describe: A the original segments, B adapt segments, C optimize weights from segments, D optimize weights from fluence, E optimize weights and shapes from segments and F optimize weights and shapes from fluence, respectively.

would no longer correctly align with the PTV. The Adapt Segments method (method B) did yield improved target coverage compared to the Original Segments method, however for all cases this was below clinical criteria. This can be explained by changes in target size and shape, which for small targets can have a large impact on relative target coverage. These methods could however perform well enough for treatment sites with little inter-fraction motion and in which the patient can be accurately positioned to limit systematic error. Regardless, random error will remain and may influence the performance.

Both weight optimization and weight and shape optimization allow the use of the original segments (method C and E), or to re-optimize the fluence and perform an initial segmentation prior to these optimizations (method D and F). Comparing these options show that using a fluence re-optimization results in more favourable dosimetric values.

Fig. 4. Boxplot of the dose difference between pre-treatment and adapted plan on the 1.5 T MR-linac based on daily anatomy for each method (N = 17 lymph nodes). The bars show the upper and lower quartiles. The whiskers show the minimum and maximum values, excluding outliers which are denoted with an asterisk. Method A – F describe: A the original segments, B adapt segments, C optimize weights from segments, D optimize weights from fluence, E optimize weights and shapes from segments and F optimize weights and shapes from fluence, respectively.

This was expected as with this method it is possible to more accurately incorporate the daily target definition.

Using weight optimization could be suitable for treatment sites with little inter-fraction motion and large treatment volumes in which more advanced methods take too long. As this method does not alter the shape of the segments, changes in size and shape of the target are not accounted for. Therefore it might be less suitable for tumor sites in which large inter-fraction changes can occur such as cervix [34] or prostate [35]. Plan adaptation using segment shape and weight optimization yields the best results.

Method F is equal to a full online replanning on the actual anatomy which was also done during the 1.5 T MR-linac first-in-man study [9]. Full online replanning, in which a completely new plan is generated on the daily anatomy without taking pre-treatment data into account, is the preferred method, as it optimally takes daily anatomy information into account. Although this method takes relatively long (on average two minutes) compared to the first four methods described in this study, applying this strategy for daily online replanning of lymph node oligometastases is feasible time-wisely when comparing to implementations of online adaptive radiotherapy by other institutions [14]. It is important to reduce the time between daily image acquisition and start of the treatment as organ motion may increase over time [36] and to ensure patient comfort.

For one particular plan it was not possible to meet the clinical dose criteria during pre-treatment planning. It was not able to obtain sufficient PTV coverage, due to overlap of the PTV and OAR adjacent to the target. Performing plan adaptation for this particular situation did also not result in acceptable treatment plans, this resulting in the outliers presented in Fig. 3. The close vicinity of OAR relative to the target, and therewith inability to create an acceptable treatment plan, may be indicative for the inability to create acceptable plans during online adaptive treatment.

The main challenge of plan adaptation for lymph node oligometastases is to achieve sufficient PTV coverage, which was not always possible using the faster plan adaptation methods. For treatment of lymph node oligometastases, in which the targets are relatively small, this can be explained as even a slight misalignment between the treatment plan and the target will have a relatively large impact. For other sites with larger target volumes, this is expected to be less problematic, and the faster plan adaptation methods might perform sufficiently. This will need to be investigated in tumour site specific studies.

A limitation of this study is that the patient data consisted only of female patients who underwent chemo-radiotherapy. The chemo-radiotherapy might result in larger changes of the target volume and shape between pre-treatment and online imaging compared to patients which are being treated for oligo metastatic disease in our clinic. However, the latter patient group does not receive additional imaging. Because of the palliative intent of this treatment, we do not want to place any additional load on these patients. Regardless, the positive treated lymph nodes of the patient group we used is representative for the position of lymph node oligometastases in the pelvic area as treated in our clinic. As it is expected for lymph nodes and surrounding OARs to behave similar in oligometastatic state we believe that the data is suitable to perform this analysis and gives us confidence to further implement this in our clinical workflow.

The clinical dose criteria for the OARs used in this study primarily focus on high dose regions, where most toxicity occurs [14]. Looking more closely at the pre-treatment and adapted plans, it can be seen that due to steep dose gradients, high dose regions only occur in the close vicinity of the target. For this reason it appears sufficient to limit the online re-contouring to a small region, as has been observed and proposed in several recent studies [37,38]. Such an approach can lead to a reduction in total treatment time or may free up additional time for other processes such as plan adaptation and allow for fast adaptive replanning [39]. Limiting the online re-contouring of OAR to a small region requires the use of absolute dose constraints.

Recent studies have shown initial benefits and feasibility of MR-guided online adaptive radiotherapy. A case study by Tyrant et al. showed the necessity of online plan adaptation for all fractions because of inter-fraction motion of the stomach [40]. A phase I trial on MR-guided online adaptive radiotherapy for the treatment of oligometastatic or unresectable primary malignancies of the abdomen resulted in online adaptive replanning for 81/97 fractions due to initial plan violation of OAR constraints (61/97) or opportunity for PTV dose escalation (20/97) [22].

For specific tumour sites in which plan adaptation has to be performed on larger target volumes, calculation time will increase, dependant on which plan adaptation method is used. This could potentially mean that the methods which include segment shape optimization will no longer be feasible within a time-span suitable for online adaptive treatment and that therefore another method must be used. Increasing optimization time potentially increases temporally dependant intra-fraction motion, requiring either larger treatment margins, motion mitigation protocols or additional plan adaptation [41,42]. A combination of large deforming target volumes, OARs in the vicinity of the target and the presence of inter-fraction motion might therefore be challenging. The most suitable methods and limitations for online plan adaptation are best investigated per treatment type. Ideally, a combination of real-time intra-fraction MRI, automatic contouring, tracking and real-time adaptive replanning should be utilized to fully benefit from MR guidance [43,44].

In conclusion, multiple plan adaptation methods, based on plan adaptation on the daily anatomy, are feasible for MR-guided SBRT of lymph node oligometastases. The most advanced method, in which a full online replanning is performed by segment shape and weight optimization after a full fluence optimization, performs as good as pre-treatment planning, yields the most favourable dosimetric values and can be performed within a time-frame acceptable for MR-guided treatment.

#### Conflict of interest statement

The authors have no conflict of interest to declare.

#### Acknowledgments

The authors wish to thank the Dutch Cancer Society for their financial support (Grant 2015-0848).

#### Appendix A. Supplementary material

Supplementary data to this article can be found online at <https://doi.org/10.1016/j.phro.2019.02.003>.

#### References

- [1] Verellen D, De Ridder M, Linthout N, Tournel K, Soete G, Storme G. Innovations in image-guided radiotherapy. *Nat Rev Cancer* 2007;7:949–60. <https://doi.org/10.1038/nrc2288>.
- [2] Jaffray DA, Siewerdsen JH, Wong JW, Martinez AA. Flat-panel cone-beam computed tomography for image-guided radiation therapy. *Int J Radiat Oncol Biol Phys* 2002;53:1337–49. [https://doi.org/10.1016/S0360-3016\(02\)02884-5](https://doi.org/10.1016/S0360-3016(02)02884-5).
- [3] Antonuk LE. Electronic portal imaging devices: a review and historical perspective of contemporary technologies and research. *Phys Med Biol* 2002;47:R31–65. <https://doi.org/10.1088/0031-9155/47/6/201>.
- [4] Litzenberg D, Dawson LA, Sandler H, Sanda MG, McShan DL, Ten Haken RK, et al. Daily prostate targeting using implanted radiopaque markers. *Int J Radiat Oncol Biol Phys* 2002;52:699–703. [https://doi.org/10.1016/S0360-3016\(01\)02654-2](https://doi.org/10.1016/S0360-3016(01)02654-2).
- [5] Purdie TG, Bissonnette JP, Franks K, Bezjak A, Payne D, Sie F, et al. Cone-beam computed tomography for on-line image guidance of lung stereotactic radiotherapy: localization, verification, and intrafraction tumor position. *Int J Radiat Oncol Biol Phys* 2007;68:243–52. <https://doi.org/10.1016/j.ijrobp.2006.12.022>.
- [6] Dehnad H, Nederveen AJ, van der Heide UA, van Moerselaar RJA, Hofman P, Lagendijk JJW. Clinical feasibility study for the use of implanted gold seeds in the prostate as reliable positioning markers during megavoltage irradiation. *Radiation Oncol*. 2003;67:295–302. [https://doi.org/10.1016/S0167-8140\(03\)00078-1](https://doi.org/10.1016/S0167-8140(03)00078-1).
- [7] Acharya S, Fischer-Valuck BW, Kashani R, Parikh P, Yang D, Zhao T, et al. Online magnetic resonance image guided adaptive radiation therapy: first clinical applications. *Int J Radiat Oncol Biol Phys*. 2016;94:394–403. <https://doi.org/10.1016/j.ijrobp.2015.10.015>.
- [8] Mutic S, Dempsey JF. The ViewRay system: magnetic resonance-guided and controlled radiotherapy. *Semin Radiat Oncol*. 2014;24:196–9. <https://doi.org/10.1016/j.semradonc.2014.02.008>.
- [9] Raaymakers BW, Jurgenliemk-Schulz IM, Bol GH, Glitzner M, Kotte A, van Asselen B, et al. First patients treated with a 1.5 T MRI-Linac: clinical proof of concept of a high-precision, high-field MRI guided radiotherapy treatment. *Phys Med Biol*. 2017;62:L41–50. <https://doi.org/10.1088/1361-6560/aa9517>.
- [10] Barillot I, Reynaud-Bougnoux A. The use of MRI in planning radiotherapy for gynaecological tumours. *Cancer Imaging* 2006;6:100–6. <https://doi.org/10.1102/1470-7330.2006.0016>.
- [11] Noel CE, Parikh PJ, Spencer CR, Green OL, Hu Y, Mutic S, et al. Comparison of onboard low-field magnetic resonance imaging versus onboard computed tomography for anatomy visualization in radiotherapy. *Acta Oncol* 2015;54:1474–82. <https://doi.org/10.3109/0284186X.2015.1062541>.
- [12] Lagendijk JJW, Raaymakers BW, Raaijmakers AJE, Overweg J, Brown KJ, Kerkhof EM, et al. MRI/linac integration. *Radiation Oncol*. 2008;86:25–9. <https://doi.org/10.1016/j.radonc.2007.10.034>.
- [13] Winkel D, Bol GH, Kiekebosch IH, Van Asselen B, Kroon PS, Jurgenliemk-Schulz IM, et al. Evaluation of online plan adaptation strategies for the 1.5T MR-linac based on “First-In-Man” treatments. *Cureus* 2018;10:e2431. <https://doi.org/10.7759/cureus.2431>.
- [14] Lamb J, Cao M, Kishan A, Agazaryan N, Thomas DH, Shaverdian N, et al. Online adaptive radiation therapy: implementation of a new process of care. *Cureus* 2017;9:e1618. <https://doi.org/10.7759/cureus.1618>.
- [15] Yeung R, Hamm J, Liu M, Schellenberg D. Institutional analysis of stereotactic body radiotherapy (SBRT) for oligometastatic lymph node metastases. *Radiat Oncol* 2017;12:105. <https://doi.org/10.1186/s13014-017-0820-1>.
- [16] Baumann R, Koncz M, Luetzen U, Krause F, Dumst J. Oligometastases in prostate cancer: metabolic response in follow-up PSMA-PET-CTs after hypofractionated IGRT. *Strahlenther Onkol*. 2018;194:318–24. <https://doi.org/10.1007/s00066-017-1239-1>.
- [17] Loi M, Frelinghuysen M, Klass ND, Oomen-De Hoop E, Granton PV, Aerts J, et al. Locoregional control and survival after lymph node SBRT in oligometastatic disease. *Clin Exp Metastasis* 2018. <https://doi.org/10.1007/s10585-018-9922-x>.
- [18] Benedict SH, Yenice KM, Followill D, Galvin JM, Hinson W, Kavanagh B, et al. Stereotactic body radiotherapy: the report of AAPM Task Group 101. *Med Phys* 2010;37:4078–101. <https://doi.org/10.1118/1.3438081>.
- [19] Park HJ, Chang AR, Seo Y, Cho CK, Jang WI, Kim MS, et al. Stereotactic body radiotherapy for recurrent or oligometastatic uterine cervix cancer: a cooperative study of the Korean radiation oncology group (KROG 14–11). *Anticancer Res* 2015;35:5103–10.
- [20] Winkel D, Kroon PS, Werensteijn-Honingh AM, Bol GH, Raaymakers BW, Jurgenliemk-Schulz IM. Simulated dosimetric impact of online replanning for stereotactic body radiation therapy of lymph node oligometastases on the 1.5T MR-linac. *Acta Oncol* 2018;57:1705–12. <https://doi.org/10.1080/0284186X.2018.1512152>.
- [21] Schippers MG, Bol GH, de Leeuw AA, van der Heide UA, Raaymakers BW, Verkooijen HM, et al. Position shifts and volume changes of pelvic and para-aortic nodes during IMRT for patients with cervical cancer. *Radiation Oncol* 2014;11:1442–5. <https://doi.org/10.1016/j.radonc.2014.05.013>.
- [22] Henke L, Kashani R, Robinson C, Curcuru A, DeWees T, Bradley J, et al. Phase I trial of stereotactic MR-guided online adaptive radiation therapy (SMART) for the treatment of oligometastatic or unresectable primary malignancies of the abdomen.

- Radiother Oncol 2018;126:519–26. <https://doi.org/10.1016/j.radonc.2017.11.032>.
- [23] Henke L, Kashani R, Yang D, Zhao T, Green O, Olsen L, et al. Simulated online adaptive magnetic resonance-guided stereotactic body radiation therapy for the treatment of oligometastatic disease of the abdomen and central thorax: characterization of potential advantages. *Int J Radiat Oncol Biol Phys* 2016;96:1078–86. <https://doi.org/10.1016/j.ijrobp.2016.08.036>.
- [24] Verkooijen HM, Kerkmeijer LGW, Fuller CD, Huddart R, Faivre-Finn C, Verheij M, et al. R-IDEAL: a framework for systematic clinical evaluation of technical innovations in radiation oncology. *Front Oncol* 2017;7:59. <https://doi.org/10.3389/fonc.2017.00059>.
- [25] Seravalli E, van Haaren PMA, van der Toorn PP, Hurkmans CW. A comprehensive evaluation of treatment accuracy, including end-to-end tests and clinical data, applied to intracranial stereotactic radiotherapy. *Radiother Oncol* 2015;116:131–8. <https://doi.org/10.1016/j.radonc.2015.06.004>.
- [26] Gerlich AS, Van der Velden JM, Fanetti G, Zoetelief A, Eppinga WSC, Seravalli E. EP-1620: the immobilizing effect of the vacuum cushion in spinal SBRT and the impact of pain (abstr). *Radiother Oncol* 2017;123:S876–7. [https://doi.org/10.1016/S0167-8140\(17\)32055-8](https://doi.org/10.1016/S0167-8140(17)32055-8).
- [27] Ponti E, Lancia A, Ost P, Trippa F, Triggiani L, Detti B, et al. Exploring All avenues for radiotherapy in oligorecurrent prostate cancer disease limited to lymph nodes: a systematic review of the role of stereotactic body radiotherapy. *Eur Urol Focus* 2017;3:538–44. <https://doi.org/10.1016/j.euf.2017.07.006>.
- [28] Wiersema L, Borst G, Nakhaee S, Peulen H, Wiersma T, Kwint M, et al. EP-1838: first IGRT results for SBRT bone and lymph node oligometastases within the pelvic region (abstr). *Radiother Oncol*. 2017;123:S1006. [https://doi.org/10.1016/S0167-8140\(17\)32273-9](https://doi.org/10.1016/S0167-8140(17)32273-9).
- [29] Goodburn RJ, Tijssen RHN, Philippens MEP. EP- 2147: comparison of spatial-distortion maps for MRSim versus MR-Linac in the brain and pelvis at 1.5T (abstr). *Radiother Oncol* 2018;127:S1184–5. [https://doi.org/10.1016/S0167-8140\(18\)32456-3](https://doi.org/10.1016/S0167-8140(18)32456-3).
- [30] Winkel D, Kroon P, Hes J, Bol G, Raaymakers B, Jürgenliemk-Schulz I. EP-1663: automated full-online replanning of SBRT lymph node oligometastases for the MR-linac (abstr). *Radiother Oncol* 2017;123:S904. [https://doi.org/10.1016/S0167-8140\(17\)32195-3](https://doi.org/10.1016/S0167-8140(17)32195-3).
- [31] Hissoiny S, Raaijmakers AJ, Ozell B, Despres P, Raaymakers BW. Fast dose calculation in magnetic fields with GPUMCD. *Phys Med Biol* 2011;56:5119–29. <https://doi.org/10.1088/0031-9155/56/16/003>.
- [32] Wells 3rd WM, Viola P, Atsumi H, Nakajima S, Kikinis R. Multi-modal volume registration by maximization of mutual information. *Med Image Anal* 1996;1:35–51. [https://doi.org/10.1016/S1361-8415\(01\)80004-9](https://doi.org/10.1016/S1361-8415(01)80004-9).
- [33] Ahunbay EE, Peng C, Chen GP, Narayanan S, Yu C, Lawton C, et al. An on-line replanning scheme for interfractional variations. *Med Phys* 2008;35:3607–15. <https://doi.org/10.1118/1.2952443>.
- [34] van de Bunt L, Jürgenliemk-Schulz IM, de Kort GAP, Roesink JM, Tersteeg RJHA, van der Heide UA. Motion and deformation of the target volumes during IMRT for cervical cancer: what margins do we need? *Radiother Oncol* 2008;88:233–40. <https://doi.org/10.1016/j.radonc.2007.12.017>.
- [35] Wu J, Haycocks T, Alasti H, Ottewell G, Middlemiss N, Abdollell M, et al. Positioning errors and prostate motion during conformal prostate radiotherapy using on-line isocentre set-up verification and implanted prostate markers. *Radiother Oncol* 2001;61:127–33. [https://doi.org/10.1016/S0167-8140\(01\)00452-2](https://doi.org/10.1016/S0167-8140(01)00452-2).
- [36] Pang EPP, Knight K, Fan Q, Tan SXF, Ang KW, Master Z, et al. Analysis of intra-fraction prostate motion and derivation of duration-dependent margins for radiotherapy using real-time 4D ultrasound. *Phys Imag Radiat Oncol* 2018;5:102–7. <https://doi.org/10.1016/j.phro.2018.03.008>.
- [37] Brunner TB, Nestle U, Grosu A-L, Partridge M. SBRT in pancreatic cancer: What is the therapeutic window? *Radiother Oncol*. 2015;114:109–16. <https://doi.org/10.1016/j.radonc.2014.10.015>.
- [38] Palacios MA, Bohoudi O, Bruynzeel AME, vanSörsen de Koste JR, Cobussen P, Slotman BJ, et al. Role of daily plan adaptation in MR-guided stereotactic ablative radiation therapy for adrenal metastases. *Int J Radiat Oncol Biol Phys* 2018;102:426–33. <https://doi.org/10.1016/j.ijrobp.2018.06.002>.
- [39] Bohoudi O, Bruynzeel AME, Senan S, Cuijpers JP, Slotman BJ, Lagerwaard FJ, et al. Fast and robust online adaptive planning in stereotactic MR-guided adaptive radiation therapy (SMART) for pancreatic cancer. *Radiother Oncol* 2017;125:439–44. <https://doi.org/10.1016/j.radonc.2017.07.028>.
- [40] Tyran M, Cao M, Raldow AC, Dang A, Lamb J, Low DA, et al. Stereotactic magnetic resonance-guided online adaptive radiotherapy for oligometastatic breast cancer: a case report. *Cureus* 2018;10:e2368. <https://doi.org/10.7759/cureus.2368>.
- [41] Kotte AN, Hofman P, Lagendijk JJ, van Vulpen M, van der Heide UA. Intrafraction motion of the prostate during external-beam radiation therapy: analysis of 427 patients with implanted fiducial markers. *Int J Radiat Oncol Biol Phys* 2007;69:419–25. <https://doi.org/10.1016/j.ijrobp.2007.03.029>.
- [42] Cramer AK, Haile AG, Ognjenovic S, Doshi TS, Reilly WM, Rubinstein KE, et al. Real-time prostate motion assessment: image-guidance and the temporal dependence of intra-fraction motion. *BMC Med Phys* 2013;13:4. <https://doi.org/10.1186/1756-6649-13-4>.
- [43] Pathmanathan AU, van As NJ, Kerkmeijer LGW, Christodouleas J, Lawton CAF, Vesprini D, et al. Magnetic resonance imaging-guided adaptive radiation therapy: a “game changer” for prostate treatment? *Int J Radiat Oncol Biol Phys* 2018;100:361–73. <https://doi.org/10.1016/j.ijrobp.2017.10.020>.
- [44] Kontaxis C, Bol GH, Stemkens B, Glitzner M, Prins FM, Kerkmeijer LGW, et al. Towards fast online intrafraction replanning for free-breathing stereotactic body radiation therapy with the MR-linac. *Phys Med Biol* 2017;62:7233–48. <https://doi.org/10.1088/1361-6560/aa82ae>.